



Scaling and interference in the dissociation of halo nuclei

M.S. Hussein^a, R. Lichtenthäler^a, F.M. Nunes^b, I.J. Thompson^{c,*}

^a Instituto de Física, Universidade de São Paulo, C.P. 66318, 05315-970 São Paulo, SP, Brazil

^b National Superconducting Cyclotron Laboratory, Michigan State University, East Lansing, MI 48824-1321, USA

^c Physics Department, University of Surrey, Guildford, Surrey GU2 7XH, UK

Received 5 June 2006; accepted 19 July 2006

Available online 2 August 2006

Editor: J.-P. Blaizot

Abstract

The dissociation of halo nuclei through their collision with light and heavy targets is considered within the continuum discretized coupled channels theory. We study the one-proton halo nucleus ${}^8\text{B}$ and the one-neutron halo nucleus ${}^{11}\text{Be}$, as well as the more normal ${}^7\text{Be}$. The procedure previously employed to extract the Coulomb dissociation cross section by subtracting the nuclear one is critically assessed, and the scaling law usually assumed for the target mass dependence of the nuclear breakup cross section is also tested. It is found that the nuclear breakup cross section for halo nuclei scales with the mass of the target as $A_T^{1/3}$. However, it does not follow the same geometrical dependence found in non-halo nuclei such as ${}^7\text{Be}$. We find further that we cannot ignore Coulomb-nuclear interference effects, which may be constructive or destructive in nature, and so the errors in previously extracted $B(E1)$ using the subtraction procedure are almost certainly underestimated.

© 2006 Elsevier B.V. Open access under [CC BY license](#).

PACS: 25.60.Dz; 25.70.De; 24.10.Eq

The study of electromagnetic dissociation of halo nuclei is an important area that supplies invaluable information about their multipole responses and consequently the details of their structure [1,2]. The theory usually employed for the purpose is the relativistic Coulomb excitation theory developed by Winther and Alder [1,3] which hinges on the Fermi–Weiszäcker–Williams (FWW) virtual photon method. Since the measurement of the dissociation cross section supplies the combined Coulomb and nuclear contributions, one is forced to subtract the latter. The common prescription employed for this subtraction procedure is the so-called scaling law: the nuclear breakup cross section should scale linearly with the radius of the target, and thus by measuring the cross section for the breakup of the halo nucleus in the predominantly nuclear field of a light target, one attempts to extrapolate to heavy targets assuming the validity of the scaling law. The Coulomb dissociation cross section for the halo nucleus on the heavy target

is then simply obtained by subtracting from the experimental cross section an extrapolated nuclear one calculated according to some prescription. It is this “nuclear-free” cross section which is fitted by the FWW result in order to extract the $B(EL)$ distribution [4–17].

Two factors convinced us to critically assess this procedure. Several theorists [18–23] have recently cast doubt on the relative importance of the nuclear contribution to the dissociation cross section, claiming in some cases that this contribution can be significantly larger than the Coulomb contribution in as heavy a target as lead, invalidating the scaling law. The second important factor is the need to supply a quantitative assessment of the Coulomb-nuclear interference terms in the cross section.

The purpose of this Letter is to settle these issues by performing a full continuum discretized coupled channels calculation for ${}^8\text{B}$, ${}^{11}\text{Be}$ and ${}^7\text{Be}$ dissociations in the fields of light-, medium- and heavy-mass targets at three laboratory energies where data are available.

Coupled channels calculations were therefore performed to calculate the elastic breakup (also called diffraction dissociation) arising in a three-body model consisting of a two-body

* Corresponding author.

E-mail address: i.thompson@surrey.ac.uk (I.J. Thompson).

Table 1
Optical and binding potential parameters for ^8B and ^{11}Be projectiles

Pair	V MeV	r_0 fm	a fm	W MeV	r_i fm	a_i fm
$p + T$	46.979	1.17	0.75	6.98	1.32	0.60
$^7\text{Be} + T$	114.2	1.0	0.85	9.44	1.30	0.81
$n + T$	37.14	1.17	0.75	8.12	1.26	0.58
$^{10}\text{Be} + T$	46.92	1.204	0.53	23.5	1.33	0.53
$n + ^{10}\text{Be}$	51.51	1.39	0.52			
partial waves pdf	28.38	1.39	0.52	V_{so}	r_{so}	a_{so}
$p + ^7\text{Be}$	44.675	1.25	0.52	4.9	1.25	0.52

projectile incident on an inert target [24,25]. Between the target and each of the two projectile components we specify optical potentials whose imaginary parts describe the loss of flux to channels beyond elastic breakup. Clearly all higher order effects are taken into account in our calculation.

For both ^8B and ^{11}Be , projectile states were included for relative motion up to partial waves $\ell_{\text{max}} = 3$ and energy $\epsilon_{\text{max}} = 10$ MeV. This energy range was divided into 20 bins when $\ell = 0$ for ^8B and when $\ell = 0, 1$ for ^{11}Be . There were 10 bins when $\ell = 1, 2$ for ^8B and $\ell = 2$ for ^{11}Be , and 5 bins in the remaining partial waves, all evenly spaced in momentum k . The coupled channels for the scattering of the projectile on the target were solved up to $R_{\text{max}} = 500$ fm, and for partial waves up to $K R_{\text{max}}$ where K is the wave number for the incident beam. The optical potentials have the same parameters for all energies, as given in Table 1, using radii calculated with an $A^{1/3}$ contribution from the target mass number. We thus impose a regular target scaling in the radial geometry of the component-target potentials, in order to examine the contributions from varying target size and varying dynamical conditions.

The results of the integrated nuclear breakup cross sections obtained from the CDCC calculations are shown in Fig. 1: circles and squares for ^8B at $E_{\text{lab}} = 44$ and 70 MeV/n respectively, left-triangle, down-triangle and right triangle for ^{11}Be at $E_{\text{lab}} = 44, 70,$ and 200 MeV/n respectively, and full diamonds for ^7Be at 100 MeV/n (after [26]). These are plotted as functions of the cubic root of the mass of the target nucleus, which is proportional to the target's radius.

Since the total reaction cross section is given by $\sigma_R = \pi/k^2 \sum_{l=0}^{\infty} (2l+1) T_l$, where T_l is the transmission coefficient and k is the wave number of relative motion, we first derive an estimate of the contribution σ_D of direct reactions in σ_R . We find this as $\sigma_D = \pi/k^2 [\sum_{l=L_g+\Delta/2}^{\infty} (2l+1) - \sum_{l=L_g-\Delta/2}^{\infty} (2l+1)]$, where Δ measures the width in angular momentum space where these peripheral reactions reside, and a step function for T_l is assumed for simplicity. We get immediately $\sigma_D = \pi/k^2 [(L_g + \Delta/2)^2 - (L_g - \Delta/2)^2]$. Since for the heavy ion systems and energies under discussion, $L_g \gg \Delta$, we find

$$\sigma_D = \frac{2\pi}{k^2} \Delta \cdot L_g. \quad (1)$$

It is expected on general simple physical arguments that Δ behaves as $\Delta = ka$, where a is a length parameter that generally depends on the bombarding energy. In fact, more detailed analysis based on the Glauber-eikonal model for T_l , which re-

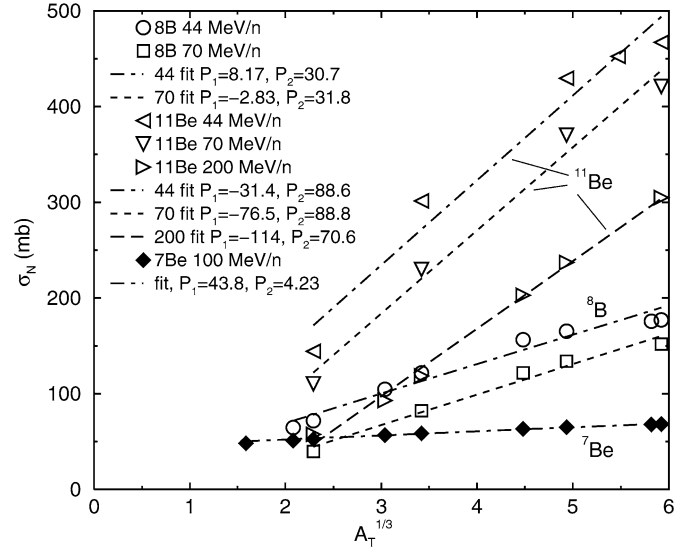


Fig. 1. Elastic nuclear breakup cross section for ^8B , ^{11}Be and ^7Be projectiles at the indicated energies, as a function of target mass number A_T , along with linear fits.

lates it to the medium-modified nucleon–nucleon cross section [27], clearly identifies a small energy dependence of a . The grazing angular momentum L_g behaves as $L_g = k(R_P + R_T)$, where $R_P + R_T$ is the sum of the projectile and target radii. Accordingly, we have

$$\sigma_D = 2\pi a(R_P + R_T). \quad (2)$$

With the same approximation for T_l , the total reaction cross section containing both central and peripheral processes comes as usual out to be

$$\sigma_R = \frac{\pi}{k^2} (L_g + 1)^2 \simeq \frac{\pi}{k^2} L_g^2 \quad (3)$$

or

$$\sigma_R = \pi(R_P + R_T)^2. \quad (4)$$

It is thus clear that while σ_R scales as the surface area of a circular disk whose radius is the sum of the radii of the interacting nuclei, σ_D , on the other hand, scales as the radius of this disc. It thus represents a circular ring of width a . This is the scaling law believed to be operative for peripheral reactions [27,28], and is also exactly the Serber model [29] for nuclear breakup, previously employed by Kobayashi et al. [30] to analyse ^{11}Li dissociation. It is also the basis of several previous analyses [4] of the breakup of one-neutron halo nuclei such ^{19}C . Note that both Eqs. (3), (4), which do not show explicit energy-dependence, are based on a geometrical model of T_l . More detailed analyses [31] based on the Glauber-eikonal model for T_l , which relate them to the medium-modified nucleon–nucleon cross section, clearly identify the quite important energy dependence of both σ_D and σ_R , but that dependence is not the subject of this Letter.

Guided by Eq. (2) above, and using $R_T = r_0 A_T^{1/3}$, we therefore anticipate the following form for the nuclear breakup cross section:

$$\sigma_N = P_1 + P_2 A_T^{1/3}, \quad (5)$$

where the parameters P_1 and P_2 (with units of mb) depend on the projectile and the structure of the target. They may also depend on the bombarding energy in accord with Glauber-eikonal models (see discussion above and [27]). We performed linear fits to the CDCC nuclear breakup cross sections as a function of $A^{1/3}$ to obtain the P_1 and P_2 shown in the legend of Fig. 1.

The nuclear breakup cross section calculated with CDCC for ^8B and ^{11}Be do show approximately the $A_T^{1/3}$ dependence of Eq. (5) as seen in Fig. 1 but do not always follow the form given by Eq. (2), in particular as, in most cases, the fits have $P_1 < 0$. The quality of the fit deteriorates considerably for $^{11}\text{Be} + ^{208}\text{Pb}$ at 44 MeV/n, possibly because of the lower energy involved and the potential influence of the bound excited $1/2^-$ state in the nuclear breakup at this energy. We should mention that our results disagree completely with those of [20], where the nuclear breakup cross section was found to scale as A_T . (In fact such a behaviour could only be possibly true for a very weakly interacting system where the whole volume of the target could be effective.)

By comparison, scaling holds for ^7Be , a normal non-halo nucleus, and Eq. (2) is fully satisfied with both P_1 and P_2 positive. The different behaviour in the nuclear scaling of ^8B and ^{11}Be could well be a manifestation of their halo nature.

The fact that the nuclear cross sections do not exactly satisfy Eq. (5) with P_1 proportional to the radius of the projectile leads us to conclude that for accurate estimates of nuclear breakup we must use realistic dynamical models, not simply Eq. (5). As well as the present CDCC model, eikonal-Glauber or time-dependent few-body procedures can be used, as done in Refs. [32–36], but as these make adiabatic (sudden) approximations about nuclear breakup and/or first-order approximations for Coulomb breakup, we use our all-order CDCC calculations for reference purposes.

The analysis of experimental data [34–36] started with the following expression for the breakup cross section:

$$\frac{d\sigma}{dE^*} = S \frac{d\sigma_C}{dE^*} + L(A_T) \frac{d\sigma(^{12}\text{C})}{dE^*}, \quad (6)$$

where S is the ground state spectroscopic factor, E^* is the excitation energy. The $d\sigma_C/dE^*$ is from the Coulomb FWW virtual photon formula, and the $d\sigma(^{12}\text{C})/dE^*$ is what is observed for a ^{12}C target. The $L(A_T)$ is a scaling factor, which may be determined either by fitting Eq. (6) to the data, exploiting the different shapes of the excitation spectra, or by calculating

$$L(A_T) = \sigma_N^{\text{th}}(A_T) / \sigma_N^{\text{th}}(^{12}\text{C}) \quad (7)$$

using eikonal-Glauber calculations of nuclear breakup $\sigma_N^{\text{th}}(A_T)$. The ^{12}C is simply a reference nucleus, and we can correct if necessary for the small Coulomb breakup it gives. Of course the above incoherent sum ignores completely Coulomb-nuclear interference effects, which we discuss further below.

In [34,35] the reaction $^{11}\text{Be} + ^{208}\text{Pb}$ at $E = 520$ MeV/n is considered. By adjusting S and L , these authors obtain $L(208) = 5.6 \pm 0.4$. This is close to our value of L , which can be extracted from Fig. 1 at $E = 200$ MeV/n, namely $L = 5.9$. Our results also agree with the eikonal-Glauber calculations of [37]. In fact, at $E = 200$ MeV/n, it has been further confirmed

to us [38] that within the eikonal formalism of [37], the value of L comes out about 5.5, very close to our model result.

On the other hand, using the same incoherent cross section formulae, Ref. [36] analyses the reaction $^{11}\text{Be} + ^{208}\text{Pb}$ at $E = 70$ MeV/n. These authors found for L the value 2.1 ± 0.5 , in accordance with the Serber model they used, which is a basis of the geometrical formula, Eq. (2), but much smaller than our result $L = 3.55$ (Fig. 1). We have, however, already shown that Eq. (2) is not valid for at least some halo nuclei. The reason for this discrepancy may reside in the neglect of the interference terms, which we see next can be rather large.

The Coulomb and nuclear potentials combine together coherently to give breakup, and the destructive interference between these potentials in the surface region is well known. If, however, the nuclear and Coulomb breakup cross sections could contribute largely to different partial waves, then the total breakup cross sections will add incoherently and Eq. (6) should be accurate.

In order to answer this question definitively at least in our test cases, we have performed further CDCC breakup calculations with both Coulomb and nuclear transition potentials as in [39,40], along with sufficient radial and partial wave limits to encompass all the resulting breakup cross sections. For reference we also performed ‘Coulomb only’ calculations, where there are no nuclear potentials at all in the transition operator. Coulomb-nuclear interference has already been examined in [32,33], but with a different motivation and using approximations applicable only in the high energy limit.

Experimentalists (e.g., [17]) often try to minimise interference problems by restrictions to small excitation energies, and/or to large impact parameters. We focus on the impact parameter restrictions, implemented by means of a maximum angle θ_{max} for integrating the cross sections over the centre of mass angle of the projectile fragments. Within semiclassical theory, this angle is related to b_{min} by $\theta_{\text{max}} = 2\eta/(kb_{\text{min}})$. We therefore use the same restrictions on our calculated breakup cross sections.

The combined Coulomb and nuclear calculation gives a total

$$\sigma_{CN} = \sigma_C + \sigma_N + \sigma_I \quad (8)$$

which defines an interference term σ_I by the difference with the sum of Coulomb-only and nuclear-only calculations. We have found that σ_I is sometimes negative (destructive interference), sometimes positive (constructive interference), and often large. Thus, although one can construct σ_N from some scaling model, the mere subtraction of it from the data would give a ‘contaminated’ Coulomb breakup cross section:

$$\hat{\sigma}_C = \sigma_C + \sigma_I = \sigma_{CN} - \sigma_N. \quad (9)$$

The use of, say, the equivalent photon method as done in [4,5] to extract the $B(E1)$ distribution for, e.g., ^8B and ^{11}Be could be questionable if σ_I is large. To ascertain typical sizes of σ_I , we first show in Fig. 2(a)–(c) the cross sections, σ_C , σ_N and σ_{CN} as the short dashed, long dashed and solid lines respectively, for the ^{11}Be and ^8B at $E_{\text{lab}} = 44$ MeV/n, and ^7Be at $E_{\text{lab}} = 100$ MeV/n, using θ_{max} corresponding to $b_{\text{min}} = 20$ fm in each case.

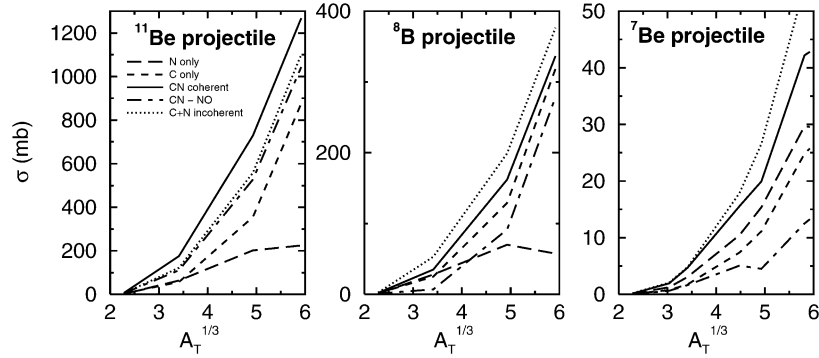


Fig. 2. Total breakup, Coulomb only, and nuclear only contributions for (a) ^{11}Be , (b) ^7Be , both at 44 MeV/n, and (c) ^7Be at 100 MeV/n, as a function of $A_T^{1/3}$. All results use scattering angle limits θ_{\max} corresponding semiclassically to $b_{\min} = 20$ fm.

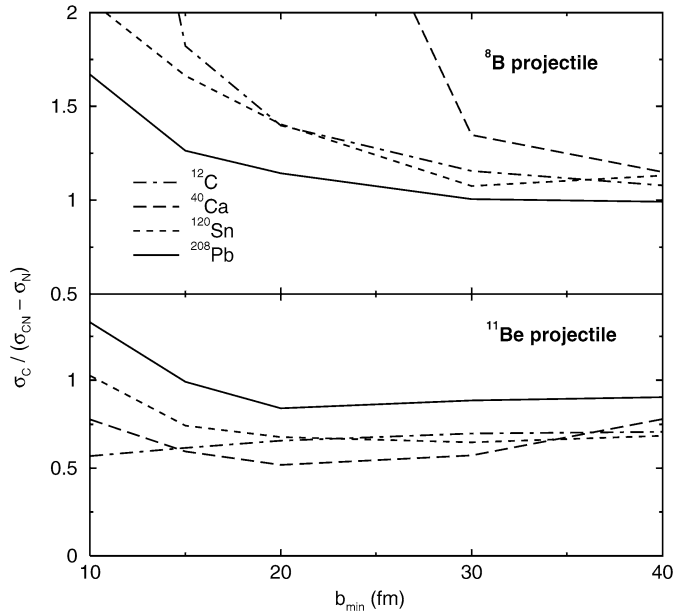


Fig. 3. Ratios of the true to the contaminated Coulomb breakup cross sections $\sigma_C / \hat{\sigma}_C = \sigma_C / (\sigma_{CN} - \sigma_N)$ as a function of the lower radial cutoff b_{\min} , for four different targets. Results for ^8B are shown in the upper panel, and for ^{11}Be in the lower panel.

To see this, in Fig. 2 we plot as the dot-dashed line the values of $\sigma_{CN} - \sigma_N$, which should ‘ideally’ agree with σ_C as the short dashed line. We also plot as the dotted line the incoherent sum $\sigma_C + \sigma_N$, whose difference from the σ_{CN} solid line indicates the effects of interference. It is evident that, for large A_T , the interference term is destructive for ^8B (the solid line $\sigma_{CN} < \sigma_{C+N}$ dotted line), so its neglect may lead to unrealistically smaller $B(E1)$ distributions. Conversely, it is constructive for ^{11}Be , yielding an unrealistically larger $B(E1)$.

In Fig. 3 we show the ratios of the ‘true’ to ‘contaminated’ Coulomb breakup cross sections $\sigma_C / \hat{\sigma}_C = \sigma_C / (\sigma_{CN} - \sigma_N)$ as a function of the lower radial cutoff b_{\min} . Ideally the ratios should be unity, but in fact we see that rarely do these values even *tend* to unity for large b_{\min} . Only for the ^8B projectile on ^{208}Pb does this occur, and the deviations from unity are worse in the ^{11}Be case. These deviations from unity indicate either that the long tail of the ^{11}Be ground state wave function gives rise to small but significant deviations from the pure Coulomb

results even at impact parameters $\gtrsim 30$ fm, or that diffraction effects are large enough to break the semiclassical connection between b_{\min} and θ_{\max} . Equivalent plots for the ^7Be projectile (not shown) give ratios far from unity, from diffraction or refraction causing nuclear breakup fragments to come out at very forward angles, implying that there is no ‘safe’ angular region where Coulomb effects dominate [26]. In general, it is clear that theoretical breakup calculations of Coulomb-nuclear interference are needed for accurate results for the breakup of ^{11}Be and ^7Be on any target.

In conclusion, we have given evidence through detailed CDCC calculations of the scaling behaviour of the nuclear breakup cross section. This cross section does approximately scale as $A_T^{1/3}$, the mass number of the target nucleus, but the scaling does not follow the geometrical form as in normal nuclei. The nuclear contribution can be as small as 1/15 of the values calculated in Refs. [18–20]. We have further calculated the ‘error’ due to the nuclear-Coulomb interference in the extracted $B(E1)$ distribution if the subtraction $\sigma_{CN} - \sigma_N$ is employed in conjunction with the virtual photon method. We believe that a full quantum calculation, including both Coulomb and nuclear potentials on equal footing, such as CDCC, is required to get credible numbers for the $B(E1)$ distribution of neutron- and proton-rich (as well as some stable) nuclei.

Acknowledgements

We acknowledge the support by the CNPq and FAPESP (Brazilian Agencies), by NSCL, Michigan State University, the National Science Foundation through grant PHY-0456656 and the UK EPSRC by grant GR/T28577.

References

- [1] C.A. Bertulani, G. Baur, Phys. Rep. 163 (1988) 299.
- [2] See, e.g., C.A. Bertulani, M.S. Hussein, G. Muenzenberg, Physics of Radioactive Ion Beams, Nova Science, 2001.
- [3] A. Winther, K. Alder, Nucl. Phys. A 319 (1979) 518.
- [4] T. Nakamura, et al., Phys. Rev. Lett. 83 (1999) 1112.
- [5] U. Datta Pramanik, et al., Phys. Lett. B 551 (2003) 63.
- [6] N. Iwasa, et al., Phys. Rev. Lett. 83 (1999) 2910.
- [7] F. Schümann, et al., Phys. Rev. Lett. 90 (2003) 232501.
- [8] P.G. Hansen, A.S. Jensen, B. Jonson, Annu. Rev. Nucl. Part. Sci. 45 (1995) 591.

- [9] I. Tanihata, Nucl. Phys. A 654 (1999) 235c.
- [10] T. Glasmacher, Annu. Rev. Nucl. Part. Sci. 48 (1998) 1.
- [11] T. Aumann, et al., Phys. Rev. C 59 (1999) 1252.
- [12] D. Sackett, et al., Phys. Rev. C 48 (1993) 118.
- [13] F. Shimoura, et al., Phys. Lett. B 348 (1995) 29.
- [14] M. Zinser, et al., Nucl. Phys. A 619 (1997) 151.
- [15] T. Nakamura, et al., Phys. Lett. B 331 (1994) 196.
- [16] A. Leistenschneider, et al., Phys. Rev. Lett. 86 (2001) 5442.
- [17] T. Nakamura, Nucl. Phys. A 734 (2004) 319.
- [18] C.H. Dasso, S.M. Lenzi, A. Vitturi, Nucl. Phys. A 639 (1998) 635.
- [19] C.H. Dasso, S.M. Lenzi, A. Vitturi, Phys. Rev. C 59 (1999) 539.
- [20] M.A. Nagarajan, C.H. Dasso, S.M. Lenzi, A. Vitturi, Phys. Lett. B 503 (2001) 65.
- [21] R. Chatterjee, R. Shyam, Phys. Rev. C 66 (2002), 061601(R).
- [22] S. Typel, R. Shyam, Phys. Rev. C 64 (2001) 024605.
- [23] V. Maddalena, R. Shyam, Phys. Rev. C 63 (2001) 051601.
- [24] I.J. Thompson, Comput. Phys. Rep. 7 (1988) 167.
- [25] N. Austern, et al., Phys. Rep. 154 (1987) 125.
- [26] N.C. Summers, F.M. Nunes, Phys. Rev. C 70 (2004), 011602(R).
- [27] J.C. Acquadro, M.S. Hussein, D. Pereira, O. Sala, Phys. Lett. B 100 (1980) 381.
- [28] W.E. Frahn, *Diffractive Processes in Nuclear Physics*, Oxford Univ. Press, Oxford, 1985.
- [29] R. Serber, Phys. Rev. 72 (1947) 1008.
- [30] T. Kobayashi, et al., Phys. Lett. B 232 (1989) 51.
- [31] M.S. Hussein, R.A. Rego, C.A. Bertulani, Phys. Rep. 201 (1991) 279.
- [32] J. Margueron, A. Bonnacorso, B.M. Brink, Nucl. Phys. A 720 (2003) 337.
- [33] A. Abu-Ibrahim, Y. Suzuki, Prog. Theor. Phys. 112 (2004) 1013.
- [34] R. Palit, et al., Phys. Rev. C 68 (2003) 034318.
- [35] T. Aumann, Eur. Phys. J. A 26 (2005) 441.
- [36] N. Fukuda, et al., Phys. Rev. C 70 (2004) 054606.
- [37] K. Hencken, G. Bertsch, H. Esbensen, Phys. Rev. C 54 (1996) 3043.
- [38] T. Aumann, private communication.
- [39] F.M. Nunes, I.J. Thompson, Phys. Rev. C 59 (1999) 2652.
- [40] J.A. Tostevin, F.M. Nunes, I.J. Thompson, Phys. Rev. C 63 (2001) 024617.